Heavy ion irradiation hardening study on 4kb arrays HfO_2-based OxRAM

Christelle Charpin-Nicolle, Nicolas Guillaume, Gauthier Lefèvre, Laurent Grenouillet, Tobias Vogel, Nico Kaiser, Eszter Piros, Stefan Petzold, C. Trautmann, Sylvain David, et al.

Heavy Ion Irradiation Hardening Study on 4kb arrays HfO_2-based OxRAM

N. Guillaume, G. Lefèvre, C. Charpin-Nicolle, L. Grenouillet, T. Vogel, N. Kaiser, E. Piros, S. Petzold, C. Trautmann, D. Sylvain, C. Vallée, L. Alff, E. Nowak

***Abstract*— HfO_2 based OxRAM devices integrated in Back End Of Line (BEOL) of 130nm CMOS have been exposed to extreme irradiation conditions related to extensive journey in space, supernova or nuclear disaster exposure: 1.635 GeV Au ion energy and very high fluences, from 10^9 ions/cm² to 10^{12} ions/cm². Single resistive devices as well as 4kbit 1T1R arrays have been studied, showing a very good resilience up to a fluence of 5.10^{10} ions/cm². For higher fluences, the degradation of access transistors is identified as the main source for information loss. Without access transistor, single 1R devices were demonstrated to be functional even at the highest fluence of 10^{12} ions/cm². TEM, EDX and nano diffraction analyses show no change in the HfO2 material, as well as in the repartition of the element in the layers, whatever the fluence. These results demonstrate the OxRAM structure is resilient to extreme irradiation conditions.**

***Index Terms*— Heavy ion irradiation, ReRAM, OxRAM, 1T1R, 4kbits arrays, Electrical characterization, TEM, nano-diffraction, EDX.**

I. INTRODUCTION

Oxide-based Resistive Random Access Memories (OxRAM), based on two resistive states, are promising candidates for replacing flash-memories, thanks to their fast switching speed, good endurance, high scalability potential and compatibility with CMOS Back-End-Of-Line (BEOL) technology. Moreover, they appear to be more resilient to radiation compared to flash memories and transistors [1-2] because the information isn't stored thanks to electric charges, and so, it could be used for space applications. Previous studies have shown the impact of the irradiation on the pristine resistance of OxRAM single cells as well as on the forming voltage, and the set voltage [3-5]. In this work, for the first time, the impact of heavy ion irradiation at fluences ranging from 10^9 ions/cm² to 10^{12} ions/cm² were investigated on 4kbit arrays: with respect to distributions of the two states (HRS and LRS) and the endurance performances. Moreover, morphological characterizations (TEM, EDX and nano-diffraction) were carried out to investigate the OxRAM structure after irradiation.

II. PREPARATION OF THE SAMPLES AND EXPERIMENTAL PROTOCOL

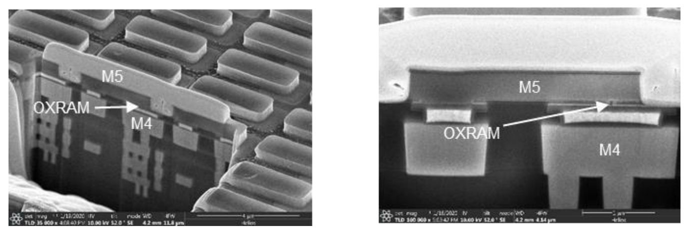

Fig. 1: FIB-SEM cross section revealing the OxRAM integration scheme

OxRAM memories were integrated in 130nm CMOS BEOL between Metal 4 (M4) and Metal 5 (M5) [Fig.1]. The transistors are NMOS types (with silicon oxide gate), and are 660 nm wide. Two types of resistive memories were fabricated: the first one is composed of a 10 nm thick HfO_2 deposited by Atomic Layer Deposition (ALD) in-between a TiN Bottom Electrode (BE) and a Ti (10 nm)/TiN Top Electrode (TE), as shown in Figure 2. In the second one, the HfO_2 active layer is Si-implanted before the deposition of Ti/TiN top layers. Si implantation (3%) induces a reduction of the pristine resistance as well as a significant reduction of the forming voltage [6]. The top and bottom electrodes have been deposited by Physical Vapor Deposition (PVD). After depositing the top electrodes, the devices have been patterned by lithography and etched to produce cells of various diameters. In this study, we focused on 400nm diameter memory dots.

OxRAM devices were programmed in three different states before being irradiated: either LRS (Low Resistance State), HRS (High Resistance State) and one third left in pristine state,

This work was funded by European commission, French State and Auvergne-Rhône Alpes region through ECSEL project WAKeMeUP and French Nano 2022 program. The work leading to this publication has received funding within the ECSEL Joint Undertaking project WAKeMeUP in collaboration with the European Union's H2020 Framework Program (H2020/2014-2020) and National Authorities, under grant agreement number 783176. Funding by the Federal Ministry of Education and Research (BMBF) under contract 16ESE0298 and by the DFG grant AL 560/21-1 is gratefully acknowledged. The irradiation experiments for this publication were performed at the UNILAC X0 beam line at the GSI Helmholtz Center for Heavy Ion Research, Darmstadt (Germany), based on a UMAT experiment in the frame of FAIR Phase-0.

N. Guillaume is with CEA, LETI, Univ. Grenoble Alpes, 38000 Grenoble, France (e-mail: nicolas.guillaume@cea.fr)

L. Grenouillet, C. Charpin-Nicolle, E. Nowak are with CEA, LETI, Univ. Grenoble Alpes, 38000 Grenoble, France.

G. Lefèvre, S. David, C. Vallée are with Université Grenoble Alpes, CNRS, CEA-LETI, LTM, F-38054 Grenoble, France

T. Vogel, N. Kaiser, E. Piros, S. Petzold, and L. Alff are with the Department Advanced Thin Film Technology, Institute of Materials Science, Technische Universität Darmstadt, Alarich-Weiss-Str.2. 64287 Darmstadt, Germany.

C. Trautmann is with the Materials Research Department, GSI Helmholtzzentrum fuer Schwerionenforschung, 64291 Darmstadt, Germany, and also with the Institute of Materials Science, Technische Universität Darmstadt, 64287 Darmstadt, Germany

corresponding to the initial state of the memory stack before any forming step. More specifically, for each 4kbit 1T1R array, 1024 devices remained in pristine state, whereas 1536 devices were programmed in LRS and 1536 devices were programmed in HRS. Forming and set voltage were applied with a gate voltage on the word line (transistor gate) such that the compliance current is about 100 µA. Electrical programming and measurements are carried out utilizing a cascade microtech bench with an Agilent B1500 parameter analyzer. Sample irradiation was performed at the UNILAC accelerator of the GSI Helmholtzzentrum (Darmstadt): Au ions were used with an energy of 1.635 GeV and three various fluences, 10^9 ions/cm², $5x10^{10}$ ions/cm² and 10^{12} ions/cm². No bias was applied during the irradiation. After irradiation, a thorough investigation has been performed: electrical measurements (4kbits resistance distribution and 10k cycles endurance), and also comparative morphological measurements: Transmission Electron Microscope (TEM), Energy Dispersive X-ray (EDX) and nano-diffraction.

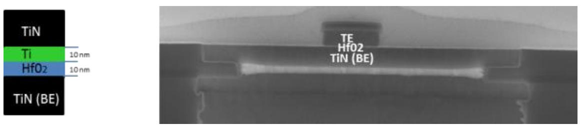

Fig. 2: Schematic Stack of the resistive memory studied (left) and SEM cross section of the stack (right).

For morphological investigation, specimens were prepared by focused ion beam etching and polishing using a FEI dual-beam Helios 450. Rough milling was applied using an operating voltage of 30kV, with subsequent reductions to 2-8kV, enabling to reduce the surface damage whereas keeping the sample with parallel sides. The TEM data were performed using a probe-corrected FEI Titan Themis at an acceleration voltage of 200kV. Nano-beam electron diffraction (NBED) was performed with a convergence semi angle α = 0.5 mrad to get diffraction spots as small as possible.

III. Results and Discussion

A. Electrical characterization

Transistors are used for the programming of OxRAM devices, providing a limitation of the current in the memories during the forming and set steps. It appears mandatory to check the functioning of the transistors after irradiation. The evolution of the drain current (Id) as function of the gate voltage and of the drain voltage (Vg and Vd respectively) has been measured before and after irradiation for the three fluences (see Figure 3).

Fig. 3 highlights the impact of irradiation on the behavior of transistors. At low fluence (10^9 ions/cm²), the transistor behavior is not impacted, regarding die to die variability. However, at higher fluences (5.10^{10} ions/cm² and especially at 10^{12} ions/cm²), a sharp decrease of the channel current is observed; moreover, the threshold voltage is clearly shifted when increasing the irradiation fluence. These results are consistent with previous results on silicon oxide gate transistor [7] : the degradation of the channel conduction is attributed to the creation of defects at the interface between the channel and the gate oxide and the increase of the threshold voltage is linked to defects induced by the irradiation within the silicon oxide itself.

Considering the deficient behavior on the transistors at the highest fluence, we first focused on the evaluation of the OxRAM 4kbit array devices after irradiation at 10^9 ions/cm² and 5.10^{10} ions/cm². Fig. 4 shows the evolution of the three states (HRS, LRS and pristine) for the two HfO_2 stacks (classic HfO_2 and Si-implanted HfO_2) after irradiation at a fluence of 10^9 ions/cm². As shown in Fig. 4a), the impact of irradiation on LRS and HRS distributions is minor: no difference is seen on HRS distribution, and only four devices over 1536 switched from HRS to LRS (HRS values that crossed the line of the highest resistance value of LRS distribution). A small shift of the pristine resistance towards a lower resistance is observed after irradiation, overall remaining in a high resistance. It is pointed out that no major difference is seen between the classic HfO_2 stack and the Si-implanted HfO_2 stack, for all distributions (HRS, LRS and pristine).

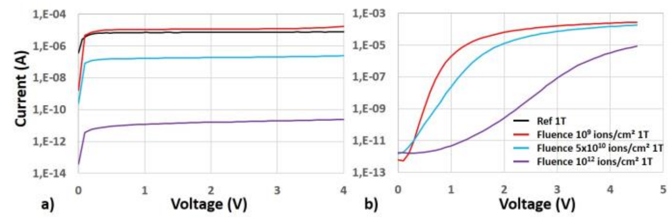

Fig. 3: Measurements carried out on single NMOS transistors (Width=660nm and Length=500nm). a) Id (Vd) at Vg=1.3V after irradiation at three various fluences (10^9 ions/cm², $5x10^{10}$ ions/cm², 10^{12} ions/cm²) and with no irradiation (reference). b) Id(Vg) at Vd=1.3V after irradiation (three fluences).

Then, endurance measurements have been performed on 4kbit irradiated arrays (see Fig. 5). The following programming conditions were applied: Vset=1.7V, Vgate_set=2.5V, Vreset=-2.5V and Vgate-reset=4.5V. A square time signal was used, trise=100ns, twidth=1µs, tfall=100ns. Endurance envelopes marked out with the quartile 1 and 3 for both HRS and LRS are shown in Fig. 5 for the two stacks (pure HfO_2 and Si-implanted HfO_2). 10k cycles endurance is achieved on both stacks, meaning the memory arrays are not impacted by the irradiation.

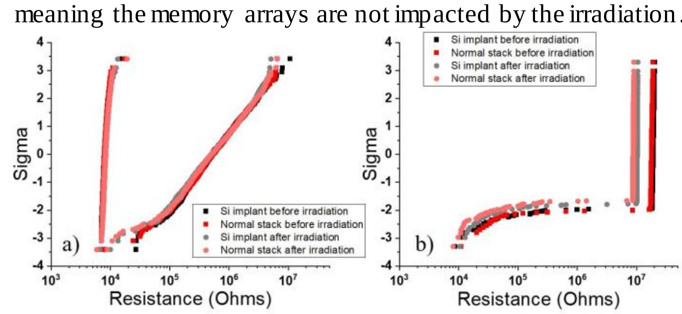

Fig. 4: LRS and HRS (a) and Pristine resistance (b) normal distribution results on two memory stacks (pure HfO_2 and Si-implanted HfO_2) after irradiation at low fluence (10^9 ions/cm²) and with no-irradiation.

After 10k cycles, HRS and LRS normal distributions are compared for three different configurations, a reference array (no irradiation), an array irradiated at the fluence of 10^9 ions/cm² and an array irradiated at the fluence $5x10^{10}$ ions/cm² [Fig. 6]. For arrays irradiated at a fluence of $5x10^{10}$ ions/cm², LRS values are slightly shifted towards higher resistance; this can be attributed to a lower current flowing at a given gate voltage (see Fig. 3).

In order to get equivalent current to that of the non-irradiated array and lowest fluence, the gate voltage was set from 2.5V to 2.75V for the classic stack and the HfO_2 Si-impacted stack [Fig. 6]. No impact on the resistance distribution is observed. In both cases, if we put aside the device failing due to intrinsic integration issues, it seems that going to a fluence of $5x10^{10}$ ions/cm² has an effect on the HRS distribution.

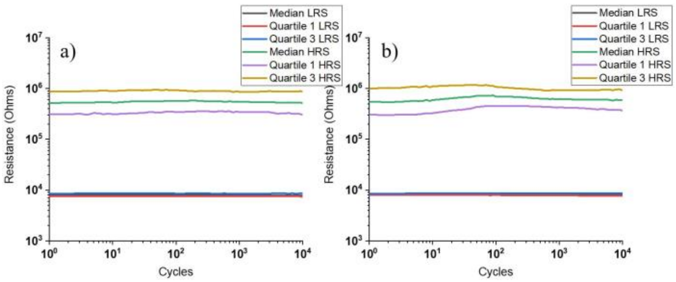

Fig. 5: 10k Cycles endurance succeeded on HfO_2 stack (a) and Si implanted HfO_2-stack (b) on 3072 devices after irradiation at a fluence of 10^9 ions/cm².

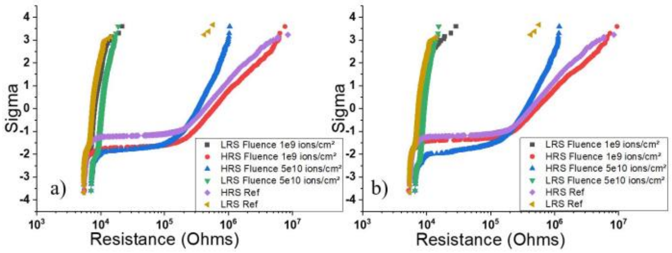

Fig. 6: Resistance distribution at the 10kth cycle for Si-implanted HfO_2 stack (a) and HfO_2 classic stack (b) with the same parameters as in Fig. 5. In the case of the classic stack, at a fluence of $5x10^{10}$ ions/cm², Vgate-set has been increased from 2.5V to 2.75V.

Since at the highest fluence, NMOS transistors are highly impacted [Fig.3] and cannot deliver sufficient current for the programming of the OxRAM devices connected in series with transistors. Therefore, single devices (1R) have been tested after irradiation at a fluence of 10^{12} ions/cm² and compared to 1R devices irradiated at the lowest fluence of 10^9 ions/cm² in their electroforming behavior in quasi-static mode [Fig. 7].

Fig.7 shows pristine resistance values which are very similar in both cases: at the reading voltage of 0.1 V, the current is roughly equal to 10^{-13} A. Anyway, an impact of the irradiation fluence can be enhanced: the shape of the current curves is somewhat different, indicating a conduction modification inside the HfO_2 active layer; this can be explained by leakage current induced by irradiation [8-9]. Moreover, forming voltages seem more spread in the case of the highest fluence compared to those in the case of the lowest fluence also increasing their mean value for the highest fluence.

Finally, a large gate width transistor (6700 nm) could be used in series with a 1R cell, so it could deliver sufficient current. Functionality of the 1R cell was demonstrated with good endurance performances reported up to 10^7 cycles (see Fig.8).

In conclusion, irradiation fluence has an impact on the subthreshold current of the 1R cells during the forming step; however, even at fluence as high as 10^{12} ions/cm², the cells are still functional, they can be formed, and even cycle when connected to a transistor which can deliver sufficient current.

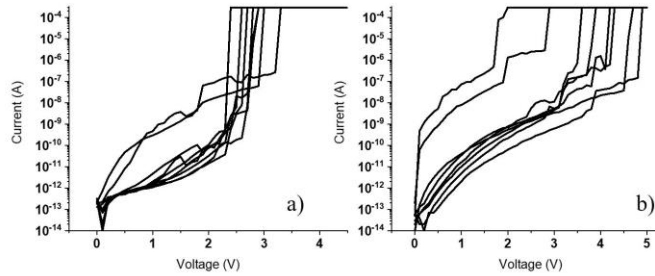

Fig. 7: Evolution of the current as function of the voltage when forming pristine OxRAM 1R devices irradiated at a fluence of 10^9 ions/cm² (a) and at a fluence of 10^{12} ions/cm² (b).

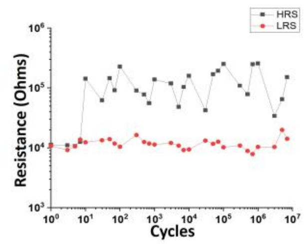

Fig. 8: 10^7 cycles performed on 1T1R HfO_2 stack. The device was irradiated at the fluence of 10^{12} ions/cm².

B. Morphological characterization

Morphological measurements were performed on three pristine OxRAM devices: a reference device (no irradiation), and two devices irradiated at the lowest and highest fluences, i.e. 10^9 ions/cm² and 10^{12} ions/cm²; Fig. 9 presents TEM images for the two irradiated samples: they are very similar, indicating same width, no distortion and no long-range order within the active layer. One can already appreciate the polycrystalline state of the upper and lower layers (titanium and titanium nitride, respectively).

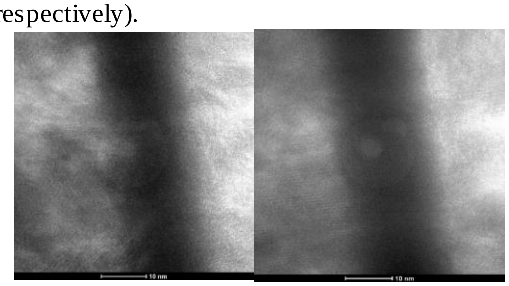

Fig. 9: TEM imaging of devices irradiated with fluence of 10^9 ions/cm² (left) and 10^{12} ions/cm² (right).

Elementary analysis by EDX was performed on the three samples [Fig. 10]: the composition as well as the distribution of the element through the active layer are identical in all cases, considering variations due to sample preparation. This indicates no noticeable interface mixing due to irradiation, with respect to a non-irradiated device.

Target damages have been simulated using the SRIM-2010 code [10] and following recommendations of Stoller et al. [11]. According to the simulation, atoms mixing is extremely limited at the interfaces in terms of depth and concentration (at the highest fluence of 10^{12} ions/cm², no more than 1 nm diffusion and 0,005% implantation respectively). This is in agreement with TEM-EDX analysis [Fig.10]. Moreover, damage calculation indicates a vacancy density of $2x10^{18}$ vacancies/cm³ (corresponding to 0.008% target damage). Neither thermal effect, nor potential contribution of channeling, nor other orientation dependent phenomena are considered in these simulations, but it has been shown that trap density of this range has an impact on the current-voltage characteristics [12] Such a low damage rate is not discernable for polycrystalline materials using TEM analysis, but is concordant with electrical characteristics changes as observed [Fig. 7]. The range and energy loss of ions in HfO_2 were estimated using SRIM. The range and energy loss of ions in HfO2 were estimated using SRIM. The calculated ion range, electronic energy loss and nuclear energy loss for 1.635 GeV Au ions in HfO2 (after passing the different covering layers) were estimated to be 38.46 µm, 52.86 keV/nm and 70.28 keV/nm, respectively.

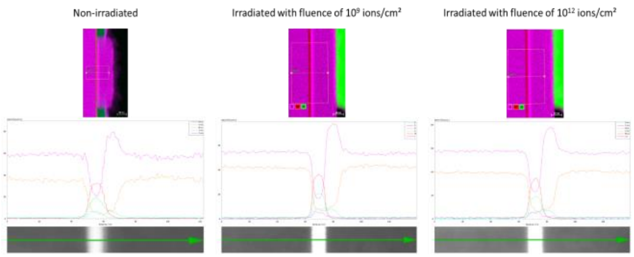

Fig. 10: Elementary profiles from EDX of a non-irradiated device and devices exposed to fluence of 10^9 ions/cm² and 10^{12} ions/cm². Elementary profiles are the same.

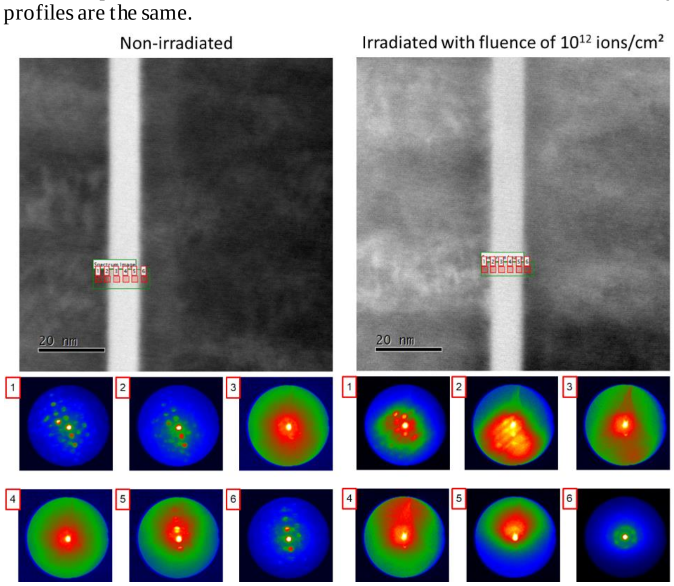

Fig. 11: Nano-diffraction patterns (bottom) of 6 areas along the active layer (indicated in the top HAADF picture) of irradiated and non-irradiated devices.

Finally, nano-diffraction measurements have been performed on irradiated and non-irradiated devices [Fig. 11]. Results are similar for all samples, indicating no detectable change in the structure. Presence of numerous diffraction spots in the TiN and Ti layers surrounding HfO2 (areas 1 and 6 in Fig. 11) points out the polycrystalline structure of these conductive layers. On the contrary, absence of clear diffraction spot in the active layer (areas 3 to 5 in Fig. 11) confirms no long-range order within the atomic structure. Nonetheless, the bright halo corresponds to very small disordered crystallites. Further analysis with improved resolution could confirm whether a phase transition occurs, as already observed [13-14].

IV. Conclusion

In this study, heavy ion irradiation has been carried out on 4kbit OxRAM arrays utilizing three fluences, 10^9 ions/cm², $5x10^{10}$ ions/cm² and 10^{12} ions/cm². Despite a degradation of the transistors for fluences over $5x10^{10}$ ions/cm², an appropriate monitoring of the programming conditions enables the functioning of 4kbits arrays: a proper memory window is maintained, even after 10k cycles. At the highest fluence, we showed 1R devices are impacted, but they were assessed to be still functionnal. TEM, EDX Nano-diffraction analyses showed no major difference between irradiated devices and non-irradiated devices, whatever fluence.

V. References

[1] *F. Tan et al., 'Investigation on the Response of TaO$_{\rm x}$-based Resistive Random-Access Memories to Heavy-Ion Irradiation', IEEE Trans. Nucl. Sci., vol. 60, no. 6, pp. 4520–4525, Dec. 2013*

[2] *D. Chen et al., 'Single-Event Effect Performance of a Commercial Embedded ReRAM', IEEE Trans. Nucl. Sci., vol. 61, no. 6, pp. 3088–3094, Dec. 2014*

[3] *M. Alayan et al., 'Experimental and Simulation Study of the Effects of Heavy-ion Irradiation on HfO2-based RRAM Cells', IEEE Trans. Nucl. Sci., pp. 1–1, 2017*

[4] *S. Petzold, S. U. Sharath, J. Lemke, E. Hildebrandt, C. Trautmann, and L. Alff, 'Heavy Ion Radiation Effects on Hafnium Oxide-Based Resistive Random Access Memory', IEEE Trans. Nucl. Sci., vol. 66, no. 7, pp. 1715–1718, Jul. 2019*

[5] *J. S. Bi et al., 'The Impact of X-Ray and Proton Irradiation on ${\rm HfO}_2/{\rm Hf}$-Based Bipolar Resistive Memories', IEEE Trans. Nucl. Sci., vol. 60, no. 6, pp. 4540–4546, Dec. 2013*

[6] *M. Barlas et al., 'Impact of Si/Al implantation on the forming voltage and pre-forming conduction modes in HfO2 based OxRAM cells', in 2016 46th European Solid-State Device Research Conference (ESSDERC), Lausanne, Switzerland, Sep. 2016, pp. 168–171*

[7] *J. R. Schwank et al., 'Radiation Effects in MOS Oxides', IEEE Trans. Nucl. Sci., vol. 55, no. 4, pp. 1833–1853, Aug. 2008*

[8] *Z. Li et al., 'Latent Reliability Degradation of Ultrathin Amorphous HfO 2 Dielectric After Heavy Ion Irradiation: The Impact of Nano-Crystallization', IEEE Electron Device Lett., vol. 40, no. 10, pp. 1634–1637, Oct. 2019*

[9] *H. L. Hughes and J. M. Benedetto, 'Radiation effects and hardening of MOS technology: devices and circuits', IEEE Trans. Nucl. Sci., vol. 50, no. 3, pp. 500–521, Jun. 2003*

[10] *J. F. Ziegler, M. D. Ziegler, and J. P. Biersack, 'SRIM – The stopping and range of ions in matter (2010)', Nuclear Instruments and Methods in Physics Research Section B: Beam Interactions with Materials and Atoms, vol. 268, no. 11–12, pp. 1818–1823, Jun. 2010*

[11] *R. E. Stoller, M. B. Toloczko, G. S. Was, A. G. Certain, S. Dwaraknath, and F. A. Garner, 'On the use of SRIM for computing radiation damage exposure', Nuclear Instruments and Methods in Physics Research Section B: Beam Interactions with Materials and Atoms, vol. 310, pp. 75–80, Sep. 2013*

[12] *V. A. Gritsenko, T. V. Perevalov, and D. R. Islamov, 'Electronic properties of hafnium oxide: A contribution from defects and traps', Physics Reports, vol. 613, pp. 1–20, Feb. 2016*

[13] *A. Benyagoub, 'Mechanism of the monoclinic-to-tetragonal phase transition induced in zirconia and hafnia by swift heavy ions', Phys. Rev. B, vol. 72, no. 9, p. 094114, Sep. 2005*

[14] *T. Vogel et al., 'Defect-induced phase transition in hafnium oxide thin films by heavy ion irradiation: The role of oxygen defects', Submitted paper to RADECS 2020*